Transition models from the quenched to ignited states for flows of inertial particles suspended in a simple sheared viscous fluid

Jean-François Parmentier, Olivier Simonin

Transition models from the quenched to ignited states for flows of inertial particles suspended in a simple sheared viscous fluid

J.-F. Parmentier[1] † **and O. Simonin**[1,2]

[1] Université de Toulouse, INPT - UPS, Institut de Mécanique des Fluides, F-31400 Toulouse, France

[2] CNRS, Institut de Mécanique des Fluides, F-31400 Toulouse, France

A review of existing theories for flows of inertial particles suspended in an unbounded sheared viscous fluid is presented first. A comparison between theoretical predictions and numerical simulation results is made for Stokes numbers from 1 to 10 in dilute and dense flows. Both particle agitation and anisotropy coefficients are examined, showing that neither of them is able to give satisfactory results in dense flows. A more precise calculation of collisional contributions to the balance law of the particle stress tensor is presented. Results of the corresponding theory are in very good agreement with numerical simulations both in dilute and dense flows.

Key words: particle/fluid flow, fluidized beds, kinetic theory

1. Introduction

Flows of inertial particles suspended in a sheared viscous fluid have been extensively studied in the last twenty years (Boelle, Balzer & Simonin 1995; Tsao & Koch 1995; Sangani *et al.* 1996; Abbas, Climent & Simonin 2009; Abbas *et al.* 2010). In dilute flows, two distinct states can exist: the quenched state, in which particles are slightly agitated, and the ignited state, in which particles are highly agitated. A transition between one state and the other was observed (Tsao & Koch 1995) when varying the particle volume fraction or the Stokes number of the flow in dilute flows. This transition was also observed in dense flows at moderate Stokes number (1 and 3.5) when varying the particle volume fraction (Abbas *et al.* 2009). Although Tsao & Koch (1995) proposed a theory to predict this transition in dilute flows, nothing exists for dense flows in which two distinct theories are needed. The present paper suggests a new theory, based on a more precise calculation of collisional contributions to the balance law of the particle stress tensor, enabling prediction of the transition between the quenched and ignited states in both dilute and dense flows. After a description of the studied case (§ 2) and a review of existing models (§§ 3 and 4), two methodologies to improve the calculation of collisional contributions are presented and model predictions are compared with numerical simulation results in terms of particle agitation and anisotropy coefficient (§ 5).

† Email address for correspondence: jf.parmentier@gmail.com

2. Case description

A simple shear flow is considered in order to validate the theoretical predictions of the particle agitation and the kinetic and collisional stress tensor as a function of the Stokes number and the solids volume fraction. Spherical particles are suspended in an infinite sheared fluid flow. The fluid velocity $\boldsymbol{U}_g(\boldsymbol{x})$ is given by:

$$\frac{\partial U_{g,i}}{\partial x_j} = \gamma \delta_{i,1}\delta_{j,3}, \tag{2.1}$$

with γ the shear rate and $\delta_{i,j}$ the Kronecker delta; γ^{-1} is the characteristic time scale of the shear. Particles are considered to be hard spheres that experience only Stokes drag and binary collisions, which is valid for low to moderate solid concentration. Between two collisions, the velocity $\boldsymbol{V}_p$ of a particle is given by Newton's laws of motion (where particle density is much greater than fluid density, $\rho_p \gg \rho_g$):

$$\frac{\mathrm{d}\boldsymbol{V}_p}{\mathrm{d}t} = -\frac{1}{\tau_p}(\boldsymbol{V}_p - \boldsymbol{U}_g(\boldsymbol{X}_p)), \tag{2.2}$$

where $\boldsymbol{X}_p$ is the position of the particle, $\tau_p = \rho_p d_p^2/(18\mu_f)$ is the Stokes relaxation time d_p is the particle diameter and μ_f is the gas dynamic viscosity. Only binary collisions are considered, without friction. The post-collision velocities $\boldsymbol{c}_a^*$ and $\boldsymbol{c}_b^*$ of colliding particles a and b are determined as functions of $\boldsymbol{c}_a$ and $\boldsymbol{c}_b$, the particle velocities at impact:

$$\boldsymbol{c}_a^* = \boldsymbol{c}_a - \tfrac{1}{2}(1+e)(\boldsymbol{g}\cdot\boldsymbol{k})\boldsymbol{k}, \tag{2.3}$$

$$\boldsymbol{c}_b^* = \boldsymbol{c}_b + \tfrac{1}{2}(1+e)(\boldsymbol{g}\cdot\boldsymbol{k})\boldsymbol{k}, \tag{2.4}$$

with $\boldsymbol{g} = \boldsymbol{c}_a - \boldsymbol{c}_b$ the particle relative velocity at the impact and $\boldsymbol{k} = (\boldsymbol{x}_b - \boldsymbol{x}_a)/d_p$ the unit vector pointing from the centre of particle a to the centre of particle b. The restitution coefficient e is the only collision parameter and will be assumed to be constant. The kinetic energy loss of the pair of particles is given by $\Delta E_c = -(1-e^2)\,(\boldsymbol{g}\cdot\boldsymbol{k})^2\,/2$.

The multibody hydrodynamic interactions are not taken into account in this study. This can be seen as a serious limitation but in fact it is not the case. The present study focuses only on collisional terms appearing in the balance law of the particle stress tensor (see § 3). As shown by Sangani *et al.* (1996), the hydrodynamic interactions can be modelled by a corrective function $R_{diss}(\alpha_p)$ applied to the Stokes drag, with α_p the particle volume fraction. In this case, collisional contributions are identical with or without hydrodynamic interactions between particles and results can be compared using an adjusted Stokes number $St_a = St/R_{diss}$.

The unbounded shear flow is an ideal case that is used here to establish and validate closure terms for collisional contributions. As will be shown in the paper, it contains sufficient physical phenomena to measure and compare the accuracy of various models. Once such models have been established and validated in this configuration, they can be applied and validated in more complex configurations, such as boundary-driven flows. However such an application is not the topic of this study.

3. Review of existing models

3.1. *General approach*

The flows of particles with finite inertia suspended in a sheared viscous fluid have been studied by Boelle *et al.* (1995), Tsao & Koch (1995) and Sangani *et al.* (1996), and more recently by Abbas *et al.* (2009) and Abbas *et al.* (2010). Such models are based on a statistical description using a Boltzmann–Liouville equation, following

Chapman & Cowling (1970):

$$\frac{\partial f_p}{\partial t} + \frac{\partial}{\partial x_i}(c_{p,i} f_p) + \frac{\partial}{\partial c_{p,i}}\left(\left\langle \frac{F_i}{m_p}\middle| \boldsymbol{V}_p = \boldsymbol{c}_p, \boldsymbol{X}_p = \boldsymbol{x}\right\rangle f_p\right) = \left(\frac{\partial f_p}{\partial t}\right)_{coll}, \tag{3.1}$$

where $f_p(\boldsymbol{c}_p, \boldsymbol{x}, t)$ is the one-particle distribution function (x being the space coordinate) and $F_i/m_p = \mathrm{d}V_{p,i}/\mathrm{d}t$ is the acceleration of a particle given by (2.2). $\langle A|B\rangle$ is the ensemble average of A conditioned by B. The right-hand side of (3.1) is the collisional rate of change of the distribution function. Equation (3.1) is not directly solved, but used to derive governing equations of the moments of f_p. The average $\langle \Psi \rangle_p$ of a function $\Psi = \Psi(\boldsymbol{c}_p, \boldsymbol{x})$ is given by:

$$n_p \langle \Psi \rangle_p = \int \Psi f_p \, \mathrm{d}\boldsymbol{c}_p, \tag{3.2}$$

where $n_p = \int f_p \, \mathrm{d}\boldsymbol{c}_p$ is the particle number density. The balance law for $\langle \Psi \rangle_p$ may be obtained by multiplying (3.1) by Ψ and a subsequent integration over the velocity phase space.

The local mean particle velocity is defined by $\boldsymbol{U}_p = \langle \boldsymbol{c}_p \rangle_p$ and the kinetic stress tensor is $R_{p,ij} = \langle C_{p,i} C_{p,j} \rangle_p$, where $\boldsymbol{C}_p = \boldsymbol{c}_p - \boldsymbol{U}_p$ is the fluctuating velocity relative to the mean velocity. Granular temperature is defined by $T = \langle C_{p,i} C_{p,i} \rangle_p / 3$. In the steady state, the particle velocity field is equal to the gas velocity field: $\boldsymbol{U}_p(\boldsymbol{x}) = \boldsymbol{U}_g(\boldsymbol{x})$ and the balance laws for the components of the kinetic stress tensor are given by:

$$n_p m_p R_{p,ik} \frac{\partial U_{p,j}}{\partial x_k} + n_p m_p R_{p,jk} \frac{\partial U_{p,i}}{\partial x_k} = -\frac{2}{\tau_p} n_p m_p R_{p,ij} + \mathbb{C}_{ij}, \tag{3.3}$$

where $\mathbb{C}_{ij}$ is the collisional rate of change of $n_p m_p R_{p,ij}$. It is defined by $\mathbb{C}_{ij} = \mathbb{C}(m_p C_{p,i} C_{p,j})$ where $\mathbb{C}(\Psi) = \int \Psi \, (\partial f_p/\partial t)_{coll} \, \mathrm{d}\boldsymbol{c}_p$ which can also be written as:

$$\mathbb{C}(\Psi) = d_p^2 \int\int\int_{\boldsymbol{g}\cdot\boldsymbol{k}>0} \delta\Psi_a f_p^{(2)}(\boldsymbol{c}_a, \boldsymbol{x}, \boldsymbol{c}_b, \boldsymbol{x} + d_p\boldsymbol{k}, t)(\boldsymbol{g}\cdot\boldsymbol{k}) \, \mathrm{d}\boldsymbol{k} \, \mathrm{d}\boldsymbol{c}_a \, \mathrm{d}\boldsymbol{c}_b, \tag{3.4}$$

where $\delta\Psi$ is the variation of Ψ during a collision, given by (2.3) and (2.4) and $f_p^{(2)}$ is the particle pair distribution function. In dilute flows, the assumption of molecular chaos is generally used to relate the pair distribution function to the one-particle velocity distribution function. In the case of high volume fraction, the radial distribution function at contact, g_0, is introduced (Chapman & Cowling 1970). In a homogeneous flow, the particle pair distribution function at contact is given by:

$$f_p^{(2)}(\boldsymbol{c}_a, \boldsymbol{x}_a, \boldsymbol{c}_b, \boldsymbol{x}_a + d_p\boldsymbol{k}, t) = g_0(\alpha_p) f_p(\boldsymbol{c}_a, \boldsymbol{x}_a, t) f_p(\boldsymbol{c}_b, \boldsymbol{x}_a + d_p\boldsymbol{k}, t), \tag{3.5}$$

where $\alpha_p = n_p m_p/\rho_p$ is the solids volume fraction.

Putting (3.5) into (3.4) and using $\boldsymbol{C}_a = \boldsymbol{c}_a - \boldsymbol{U}_p(\boldsymbol{x})$ and $\boldsymbol{C}_b = \boldsymbol{c}_b - \boldsymbol{U}_p(\boldsymbol{x} + d_p\boldsymbol{k})$ instead of $\boldsymbol{c}_a$ and $\boldsymbol{c}_b$ leads to:

$$\mathbb{C}(\Psi) = g_0 d_p^2 \int\int\int_{\boldsymbol{G}\cdot\boldsymbol{k} > \delta\boldsymbol{U}_p\cdot\boldsymbol{k}} \delta\Psi_a f_p(\boldsymbol{C}_a) f_p(\boldsymbol{C}_b)((\boldsymbol{G} - \delta\boldsymbol{U}_p)\cdot\boldsymbol{k}) \, \mathrm{d}\boldsymbol{k} \, \mathrm{d}\boldsymbol{C}_a \, \mathrm{d}\boldsymbol{C}_b. \tag{3.6}$$

The relative velocity $\boldsymbol{g} = \boldsymbol{c}_a - \boldsymbol{c}_b$ has been expressed as a function of the relative fluctuating velocity $\boldsymbol{G} = \boldsymbol{C}_a - \boldsymbol{C}_b$ using:

$$\boldsymbol{g} = \boldsymbol{G} - \delta\boldsymbol{U}_p, \tag{3.7}$$

where $\delta\boldsymbol{U}_p = \boldsymbol{U}_p(\boldsymbol{x} + d_p\boldsymbol{k}) - \boldsymbol{U}_p(\boldsymbol{x})$ is the contribution of the shear to the relative velocity of the colliding particles. In simple shear flow $\delta\boldsymbol{U}_p = \gamma d_p k_z \boldsymbol{e}_x$. The first term of the

right-hand side of (3.7) is the contribution of the particle agitation to the colliding particle relative velocity. In the simple shear flow, the particle agitation is given by the values of $\mathbb{C}_{ii}$, $\mathbb{C}_{33}$ and $\mathbb{C}_{13}$ and the set of equations (3.3) is reduced to:

$$0 = -2St\, R^*_{p,13} - 6T^* + St\, \mathbb{C}^*_{ii}, \tag{3.8a}$$

$$0 = -2R^*_{p,33} + St\, \mathbb{C}^*_{33}, \tag{3.8b}$$

$$0 = -St\, R^*_{p,33} - 2R^*_{p,13} + St\, \mathbb{C}^*_{13}, \tag{3.8c}$$

where $St = \gamma\tau_p$ is the Stokes number, and $\mathbb{C}^*_{ij} = \mathbb{C}_{ij}/(\gamma^3 a^2 n_p m_p)$, $T^* = T/(\gamma a)^2$ and $R^*_{p,ij} = R_{p,ij}/(\gamma a)^2$ are respectively the dimensionless collisional terms, particle agitation and particle stress tensor. We will focus on the prediction of T^*, $R^*_{p,33}$ and $R^*_{p,13}$ and consequently on the calculation of $\mathbb{C}^*_{ii}$, $\mathbb{C}^*_{33}$ and $\mathbb{C}^*_{13}$. In order to close the set of equations (3.8), the expression for the one-particle velocity distribution function is needed to calculate $\mathbb{C}_{ij}$.

Two distinct mechanisms cause collisions: the particle agitation, where collisions occur due to their random velocities; and the mean shear, where particles collide because the mean velocity varies at the characteristic length scale of a particle diameter. The characteristic relative velocity of two colliding particles induced by the agitation can be estimated by $\sqrt{T}$. The characteristic relative velocity of two colliding particles induced by the shear can be estimated by γa, where a is the particle radius. The first mechanism is dominant when the relative velocity between two colliding particles is mainly due to their agitation corresponding to $T^* \gg 1$, with:

$$T^* = T/(\gamma a)^2 . \tag{3.9}$$

On the other hand, the second mechanism will be dominant when the relative velocity between two colliding particles is mainly due to the shear, i.e. $T^* \ll 1$. These two limits are representative of two distinct states (Tsao & Koch 1995): the ignited state, where $T^* \gg 1$, and the quenched state, where $T^* \ll 1$. Different closures for the one-particle velocity distribution are used in these regimes in order to calculate the collisional terms $\mathbb{C}_{ij}$.

3.2. *Quenched-state theories*

When both the suspension concentration and the particle inertia are low, the relaxation time of the particle τ_p is of the same order as or lower than the average time between successive collisions τ_c. Particles have very weak velocity fluctuations as they are more likely to follow the fluid streamlines after a collision. Tsao & Koch (1995) called this specific state the quenched state, as opposed to the ignited state for agitated systems. Tsao & Koch (1995) proposed closing the collisional term (3.4) by assuming a Dirac function for the velocity distribution function:

$$f_p(\boldsymbol{c}_p, \boldsymbol{x}) = n_p \delta(\boldsymbol{c}_p - \boldsymbol{U}_p(\boldsymbol{x})). \tag{3.10}$$

Hence the relative velocity between two colliding particles is assumed to be only due to the mean shear which means that collisions induced by the particle agitation are neglected ($\boldsymbol{G} = \boldsymbol{0}$ in (3.6)). Consequently, this theory will apply when $T^* \ll 1$.

Tsao & Koch (1995) assumed perfectly elastic conditions ($e = 1$) and a dilute flow ($g_0 = 1$). These two conditions can be broken and one can simply put (3.10) into (3.6), leading for $\mathbb{C}^*_{ij}$ to:

$$\mathbb{C}^*_{ij} = \left(\frac{1+e}{2}\right)^2 \alpha_p g_0 \frac{24}{\pi} I_{ij}, \tag{3.11}$$

with I_{ij} defined by $I_{ij} = -\iint_{k_1 k_3 < 0} (k_1 k_3)^3 \, k_i k_j \, \mathrm{d}\boldsymbol{k}$. Resulting collisional terms are independent of the granular temperature; in particular, they are not null when T is null. All collisions contribute positively to the production of granular temperature which is expressed as:

$$T = \frac{128}{945\pi} \left(\frac{1+e}{2} \right)^2 \alpha_p g_0 \, (\gamma a)^2 \, St^3 \left(1 + \frac{9\pi}{16} St^{-1} + \frac{9}{2} St^{-2} \right). \tag{3.12}$$

Table 1 compares the collisional terms given by the original theory proposed by Tsao & Koch (1995) with the extended one ($e \neq 1$ and $g_0 \neq 1$). Note that the terms given by Tsao & Koch (1995) have been corrected by a factor 2 (Abbas *et al.* 2009).

3.3. *Ignited-state theories*

In the ignited state, the particles are highly agitated and between two collisions the particle velocities are only slightly affected by the drag from the surrounding gas. Following Jenkins & Richman (1985), Boelle *et al.* (1995), Tsao & Koch (1995) and Sangani *et al.* (1996) propose closing the velocity distribution function using a deviated Maxwellian (Grad 1949):

$$f_p(\boldsymbol{C}_p) = \left(1 + \frac{\widehat{R}_{p,ij}}{2T^2} C_{p,i} C_{p,j} \right) f_0(\boldsymbol{C}_p), \tag{3.13}$$

where $\widehat{R}_{p,ij} = R_{p,ij} - T\delta_{ij}$ is the anisotropic part of the kinetic stress tensor and f_0 is the Maxwellian defined by:

$$f_0 = \frac{n_p}{(2\pi T)^{3/2}} \exp\left(-\frac{\boldsymbol{C}_p^2}{2T} \right). \tag{3.14}$$

The theory of Tsao & Koch (1995) focuses on dilute flows of perfectly elastic particles ($e = 1$). The authors put (3.13) into (3.6) and assume moreover that $\boldsymbol{\delta U}_p = \boldsymbol{0}$, which means that collisions only occur due to particle agitation. Resulting expressions are given in table 1.

The theories of Boelle *et al.* (1995) and Sangani *et al.* (1996) (for moderately large St) extend the work of Tsao & Koch (1995) to dense flows. Sangani *et al.* (1996) take into account hydrodynamic interactions between particles. However, the present study focuses only on collisional terms. From this point of view, the theories of Boelle *et al.* (1995) and Sangani *et al.* (1996) are identical. They used the deviated Maxwellian (3.13) to close the velocity distribution function into (3.6). Moreover, following Jenkins & Richman (1985), they performed a first-order Taylor development of (3.6) in γ, or similarly in $\boldsymbol{\delta U}_p$. This means that shear-induced collisions have been slightly taken into account. Second-orders terms in $\widehat{R}_{p,ij}$ have been neglected. Resulting collisional terms are given in table 1.

The Tsao & Koch (1995) theory for the dilute ignited state takes into account second-order terms in $\widehat{R}_{p,ij}$, leading to a term proportional to $\widehat{R}^2_{p,13}$ in $\mathbb{C}^*_{33}$. This term is not present in the theories of Boelle *et al.* (1995) and Sangani *et al.* (1996) for the dense ignited state. However, as mentioned by Tsao & Koch (1995), the primary effect of this term is only to produce a slight difference between $R_{p,zz}$ and $R_{p,yy}$, and can be neglected. In this case, the theory of Tsao & Koch (1995) is contained in the theories of Boelle *et al.* (1995) and Sangani *et al.* (1996). The collisional terms of Tsao & Koch (1995) have only terms of $O(\sqrt{T^*}\widehat{R}^*_{p,ij})$. In the case where $e = 1$,

	$\mathbb{C}^*_{ii}$	$\mathbb{C}^*_{33}$	$\mathbb{C}^*_{13}$
Quenched state (Tsao & Koch 1995)	$\frac{128}{35\pi}\alpha_p$	$\frac{512}{315\pi}\alpha_p$	$-\frac{16}{35}\alpha_p$
Ignited state (Tsao & Koch 1995)	0	$-\frac{48}{5\sqrt{\pi}}\alpha_p\sqrt{T^*}(\widehat{R}^*_{p,33}+\frac{1}{21}\widehat{R}^2_{p,13})$	$-\frac{48}{5\sqrt{\pi}}\alpha_p\sqrt{T^*}\widehat{R}^*_{p,13}$
Linear transition theory	$+\frac{128}{35\pi}\alpha_p$	$-\frac{48}{5\sqrt{\pi}}\alpha_p\sqrt{T^*}(\widehat{R}^*_{p,33}+\frac{1}{21}\widehat{R}^2_{p,13})$	$-\frac{48}{5\sqrt{\pi}}\alpha_p\sqrt{T^*}\widehat{R}^*_{p,13}$
(Tsao & Koch 1995)		$+\frac{512}{315\pi}\alpha_p$	$-\frac{16}{35}\alpha_p$
Dense inelastic quenched-state theory	$\frac{128}{35\pi}\left(\frac{1+e}{2}\right)^2\alpha_p g_0$	$\frac{512}{315\pi}\left(\frac{1+e}{2}\right)^2\alpha_p g_0$	$-\frac{16}{35}\left(\frac{1+e}{2}\right)^2\alpha_p g_0$
Dense inelastic ignited-state theory	$-\frac{12}{\sqrt{\pi}}(1-e^2)\alpha_p g_0 T^{*3/2}$	$-\frac{4}{\sqrt{\pi}}(1-e^2)\alpha_p g_0 T^{*3/2}$	$-\frac{12}{5\sqrt{\pi}}(1+e)(3-e)\alpha_p g_0\sqrt{T^*}\widehat{R}^*_{p,13}$
(Boelle *et al.* 1995, Sangani *et al.* 1996)	$-\frac{8}{5}(1+e)\alpha_p g_0\widehat{R}^*_{p,13}$	$-\frac{12}{5\sqrt{\pi}}(1+e)(3-e)\alpha_p g_0\sqrt{T^*}\widehat{R}^*_{p,33}$	$-\frac{2}{5}(1+e)(3-e)\alpha_p g_0 T^*$
	$\frac{16}{5\sqrt{\pi}}(1+e)\alpha_p g_0\sqrt{T^*}$		$-\frac{4}{5}(1+e)\alpha_p g_0\widehat{R}^*_{p,33}$
Dense inelastic linear transition theory	$-\frac{12}{\sqrt{\pi}}(1-e^2)\alpha_p g_0 T^{*3/2}$	$-\frac{4}{\sqrt{\pi}}(1-e^2)\alpha_p g_0 T^{*3/2}$	$-\frac{12}{5\sqrt{\pi}}(1+e)(3-e)\alpha_p g_0\sqrt{T^*}\widehat{R}^*_{p,13}$
	$-\frac{8}{5}(1+e)\alpha_p g_0\widehat{R}^*_{p,13}$	$-\frac{12}{5\sqrt{\pi}}(1+e)(3-e)\alpha_p g_0\sqrt{T^*}\widehat{R}^*_{p,33}$	$-\frac{2}{5}(1+e)(3-e)\alpha_p g_0 T^*$

TABLE 1. (Continued on next page)

	$\mathbb{C}^*_{ii}$	$\mathbb{C}^*_{33}$	$\mathbb{C}^*_{13}$
Nonlinear transition theory	$\frac{16}{5\sqrt{\pi}}(1+e)\alpha_p g_0\sqrt{T^*}$	$+\frac{512}{315\pi}\left(\frac{1+e}{2}\right)^2\alpha_p g_0$	$-\frac{4}{5}(1+e)\alpha_p g_0\widehat{R}^*_{p,33}$
	$+\frac{128}{35\pi}\left(\frac{1+e}{2}\right)^2\alpha_p g_0$		$-\frac{16}{35}\left(\frac{1+e}{2}\right)^2\alpha_p g_0$
	$-\frac{12}{\sqrt{\pi}}(1-e^2)\alpha_p g_0 T^{*3/2}A_1$	$\frac{4}{\sqrt{\pi}}(1+e)((1+e)B_1$	$-\frac{12}{5\sqrt{\pi}}(1+e)(3-e)\alpha_p g_0\sqrt{T^*}\widehat{R}^*_{p,13}$
		$-2B_2)\alpha_p g_0 T^{*3/2}$	
	$-\frac{8}{5}(1+e)\alpha_p g_0\widehat{R}^*_{p,13}$	$-\frac{12}{5\sqrt{\pi}}(1+e)(3-e)\alpha_p g_0\sqrt{T^*}\widehat{R}^*_{p,33}$	$-\frac{2}{5}(1+e)(3-e)\alpha_p g_0 T^*$
	$\frac{16}{5\sqrt{\pi}}(1+e)\alpha_p g_0\sqrt{T^*}A_2$		$-\frac{4}{5}(1+e)\alpha_p g_0\widehat{R}^*_{p,33}$
			$-\frac{16}{35}\left(\frac{1+e}{2}\right)^2\alpha_p g_0$

TABLE 1. Comparison of collisional terms between the different theories.

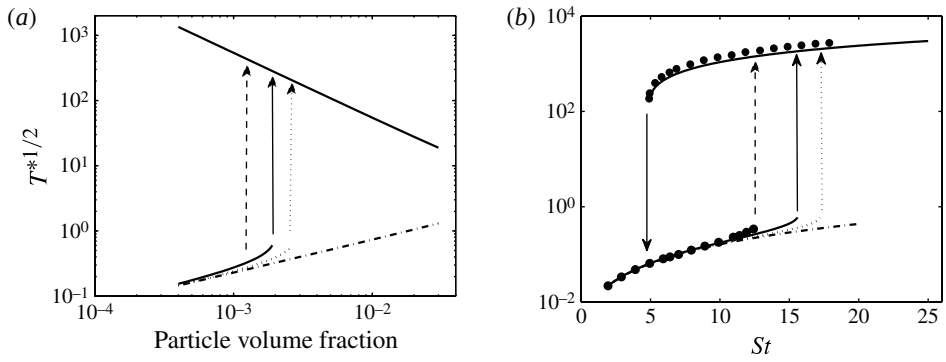

FIGURE 1. Particle agitation as a function of (a) the particle volume fraction for $St = 10$ or (b) the Stokes number for $\alpha_p = 5 \times 10^{-4}$. $e = 1$: ——, nonlinear transition theory; · · · · ··, linear transition theory (Tsao & Koch 1995); – · –·, quenched-state theory; dashed arrow: transition obtained from direct-simulation Monte Carlo method (Tsao & Koch 1995).

Boelle *et al.* (1995) and Sangani *et al.* (1996) collisional terms contained additional terms of $O(T^*)$, $O(\widehat{R}^*_{p,ij})$ and $O(\sqrt{T^*})$ (see table 1). These terms come from the first-order Taylor development in $\boldsymbol{\delta U}_p$ of (3.6) (while Tsao & Koch 1995 assume $\boldsymbol{\delta U}_p = \boldsymbol{0}$).

3.4. *Linear transition theory of Tsao & Koch (1995)*

As the quenched-state theory assumes only shear-induced collisions ($\boldsymbol{G} = \boldsymbol{0}$) and the dilute ignited-state theory assumes only variance-driven collisions ($\boldsymbol{\delta U}_p = \boldsymbol{0}$), Tsao & Koch (1995) proposed simply adding the collisional terms of the two theories to take into account both the contributions of shear-induced and variance-driven collisions, leading to linear transition. Resulting collisional terms are given in table 1.

4. Comparison to simulation results

To compare the prediction of theories with numerical simulations, the input of g_0 is needed. Following Tsao & Koch (1995), Sangani *et al.* (1996) and Abbas *et al.* (2009) the value proposed by Carnahan & Starling (1969) ($g_0 = (1 - \alpha_p/2)/(1 - \alpha_p)^3$) is used.

4.1. *Transition in dilute flows*

Using numerical simulations (the direct-simulation Monte Carlo method and periodic Lagrangian simulations of hard spheres), Tsao & Koch (1995) have shown that multiple steady states can exist for low concentrations. As shown on figure 1(a) where $St = 10$, when α_p is below a critical value $\alpha_{p,c}$, quenched or ignited states can exist depending on the initial conditions. Numerical simulations predict $\alpha_{p,c} \simeq 1.2 \times 10^{-3}$. The dilute transitional theory of Tsao & Koch (1995) is able to capture the existence of multiple steady states, but overestimates the critical particle volume fraction, leading to $\alpha_{p,c} \simeq 2.6 \times 10^{-3}$.

An hysteresis is observed when increasing the Stokes number at a fixed concentration and particle elasticity. As shown on figure 1(b) where $\alpha_p = 5 \times 10^{-4}$, if the system is in the quenched state and one increases St gradually, then the system jumps to the ignited state for $St = St_{c2} \simeq 13$. If St is decreased gradually for a system in the ignited state, the system jumps down to the quenched state for $St = St_{c1} = \sqrt{24}$.

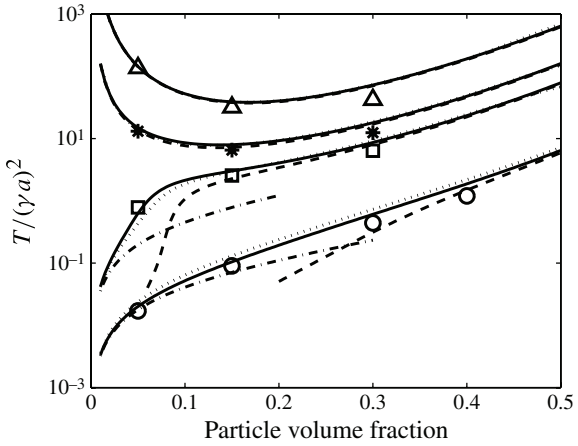

FIGURE 2. Particle agitation $T/(\gamma a)^2$ as a function of the solids volume fraction for different Stokes numbers. $\triangle$, $*$, $\square$ and $\bigcirc$: numerical simulations for $St = 10$, 5, 3.5 and 1 respectively. ——, Nonlinear theory; · · · · · ·, dense linear transition theory; – – –, dense ignited-state theory (in each case from top to bottom, $St = 10$, 5, 3.5 and 1); – · –·, dense quenched-state theory (top, $St = 3.5$ and bottom, 1).

Therefore, one may have either the ignited or quenched state for $St_{c1} < St < St_{c2}$ depending on the previous history of the shear rate experienced by the suspension. As shown on figure 1(*b*), the dilute transitional theory of Tsao & Koch (1995) is able to capture this hysteresis effect but overestimates St_{c2} by 30%, predicting a value for $St_{c2} \simeq 17$.

4.2. *Transition in dense flows*

4.2.1. *Particle agitation*

Abbas *et al.* (2009) performed periodic Lagrangian numerical simulations for $1 \leqslant St \leqslant 10$ and a volume fraction between 5 % and 30 %. Particles were perfectly elastic ($e = 1$) and no hydrodynamic interactions were taken into account. Results are shown on figure 2. When $T^* > 10$, the level of particle agitation obtained by the simulations and predicted by the dense ignited-state theory match very well (corresponding to numerical simulations for $St = 5$ and 10). The quenched-state theory underestimates the particle agitation. On the contrary, when $T^* < 10^{-2}$ the level of particle agitation is predicted well by the dense quenched-state theory, and the dense ignited-state theory drastically underestimates it (corresponding to numerical simulations for $St = 1$ and 3.5 with $\alpha_p = 5\,\%$). When $10^{-2} < T^* < 10$ a transition between the dense quenched-state theory and the dense ignited-state theory occurs.

4.2.2. *Anisotropy coefficients*

Predictions given by the different theories of the anisotropy coefficients $a_{33} = \widehat{R}_{p,33}/T$ and $a_{13} = \widehat{R}_{p,13}/T$ are plotted as functions of T^* on figures 3 ($e = 0.8$, $St = 5$), 4 ($e = 1$, $St = 3.5$) and 5 ($e = 1$, $St = 1$) and compared with Lagrangian simulation results.

While the dense inelastic ignited-state theory gives satisfactory results for the particle agitation when $St = 5$, the anisotropy coefficients can be overestimated (or

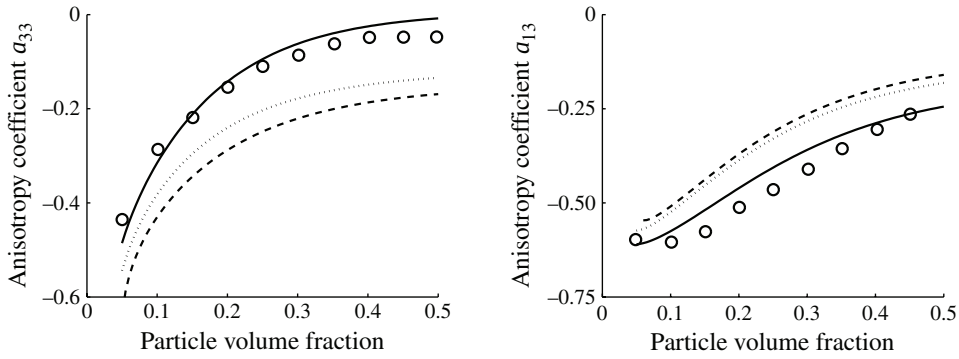

FIGURE 3. Anisotropy coefficients a_{33} and a_{13} as a function of the solids volume fraction, for $St = 5$ and $e = 0.8$. ○, Lagrangian simulations (Boelle *et al.* 1995), ——, nonlinear transition theory; · · · · ··, dense inelastic linear transition theory; – – –, dense inelastic ignited-state theory.

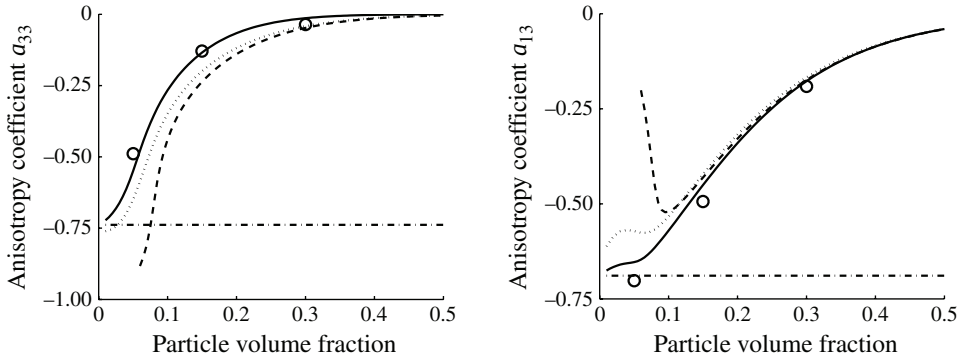

FIGURE 4. Anisotropy coefficients a_{33} and a_{13} as a function of the solids volume fraction, for $St = 3.5$ and $e = 1$: ○, Lagrangian simulations (Abbas *et al.* 2009); ——, nonlinear transition theory; · · · · ·, dense linear transition theory; – – –, dense ignited-state theory; – · –·, dense quenched-state theory.

underestimated) by up to a factor two (or one half). For $St = 1$ and 3.5 a clear transition between the dense quenched theory and dense ignited theory is observed when varying the particle volume fraction. When $\alpha_p \leqslant 5\,\%$ the dense quenched-state theory gives satisfactory results and when $\alpha_p \geqslant 30\%$ the dense ignited theory gives satisfactory results. However none of the theories is able to predict values of anisotropy coefficients during the transition.

5. Transitional theories

While the linear transition theory of Tsao & Koch (1995) gives satisfactory results in dilute flows, a single theory enabling prediction of the quenched state, the ignited state and the transition in dense flow is required. The two following sections will present two theories devoted to fulfilling this objective.

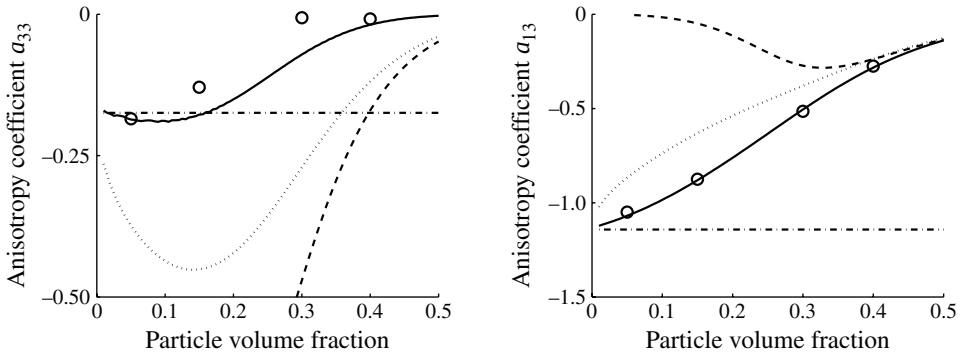

FIGURE 5. Anisotropy coefficients a_{33} and a_{13} as a function of the solids volume fraction, for $St = 1$ and $e = 1$: ○, Lagrangian simulations (Abbas *et al.* 2009); ——, nonlinear transition theory; ·····, dense linear transition theory; – – –, dense ignited-state theory; — · —·, dense quenched-state theory.

5.1. *Dense inelastic linear transition theory*

A natural idea is to extend the linear transition theory of Tsao & Koch (1995) to dense flow by simply adding the collisional terms of the dense inelastic quenched-state theory and the dense inelastic ignited theory. Resulting collisional terms are given in table 1.

In dilute flows, predictions of this theory are the same as the original linear transition theory of Tsao & Koch (1995). In dense flows, the dense linear transition theory matches very well the particle agitation predicted by numerical simulations for all particle volume fractions and all Stokes numbers (figure 2), in particular, when $10^{-2} < T^* < 10$ (corresponding to the transition), in which neither the dense quenched-state theory nor the dense ignited theory give satisfactory results. However the prediction of anisotropy coefficients is not satisfactory. For $St = 5$, anisotropy coefficients are only slightly improved (figure 3). For $St = 1$, while a satisfactory transition is obtained for a_{13}, there is a strong disagreement for a_{33} (figure 5).

5.2. *Exact contribution of the shear and the agitation to collisions*

5.2.1. *Collisional term calculation*

In the quenched-state theories, variance-driven collisions are neglected whereas shear-induced collisions are neglected in the dilute ignited-state theory. The dense state theory slightly takes into account shear-induced collisions using a first-order Taylor development in $\delta \boldsymbol{U}_p$. However, in the case of simple shear flow, the exact contribution of the shear and the agitation to collisions can be calculated if the velocity distribution function is Maxwellian. Therefore, a new closure of collisional terms is proposed in order to improve the predictions of the transition between the quenched and ignited states.

Following the ignited-state theories, the velocity distribution function is assumed to be a deviated Maxwellian:

$$f_p = f_0 + \Delta f, \tag{5.1}$$

with f_0 the Maxwellian (3.14) and $\Delta f = f_p - f_0$ with f_p given by the Grad (1949) development (3.13). Hence the collisional terms (3.6) can be decomposed into

two parts:

$$\mathbb{C}(\Psi) = \mathbb{C}_0(\Psi) + \Delta\mathbb{C}(\Psi); \tag{5.2}$$

$\mathbb{C}_0(\Psi)$ is obtained using $f_p = f_0$ in (3.6) and $\Delta\mathbb{C}(\Psi)$ using $f_p = \Delta f$. In the ignited-state theories, $\Delta\mathbb{C}(\Psi)$ corresponds to the contribution of collisional terms proportional to $\widehat{R}_{p,ij}$.

Putting $f_p = f_0$ in (3.6) and using the variables change $(\boldsymbol{C}_a, \boldsymbol{C}_b) \rightarrow (\boldsymbol{G}, \boldsymbol{Q} = (\boldsymbol{C}_a + \boldsymbol{C}_b)/2)$ leads for $\mathbb{C}_0(\Psi)$ to:

$$\mathbb{C}_0(\Psi) = \frac{g_0 d_p^2 n_p^2}{(2\pi T)^3} \int\int\int_{\boldsymbol{G}\cdot\boldsymbol{k} > \boldsymbol{\delta U}_p \cdot \boldsymbol{k}} \delta\Psi_a \exp\left(-\frac{\boldsymbol{G}^2}{4T}\right) \times \exp\left(-\frac{\boldsymbol{Q}^2}{T}\right) ((\boldsymbol{G} - \boldsymbol{\delta U}_p) \cdot \boldsymbol{k})\, \mathrm{d}\boldsymbol{G}\, \mathrm{d}\boldsymbol{Q}\, \mathrm{d}\boldsymbol{k}. \tag{5.3}$$

The integration over $\boldsymbol{Q}$, G_θ and G_ϕ can be performed, leading to:

$$\mathbb{C}_0(\Psi) = \frac{g_0 d_p^2 n_p^2}{2\sqrt{\pi T}} \int\int_{G_k > \boldsymbol{\delta U}_p \cdot \boldsymbol{k}} \delta\Psi_a \exp\left(-\frac{\boldsymbol{G}_k^2}{4T}\right) (G_k - \boldsymbol{\delta U}_p \cdot \boldsymbol{k})\, \mathrm{d}G_k\, \mathrm{d}\boldsymbol{k}. \tag{5.4}$$

where (G_k, G_θ, G_ϕ) are the projection of G in a spherical coordinate system in which $G_k = G \cdot k$. Choosing $\Delta\mathbb{C}(\Psi)$ identically to corresponding terms in the dense ignited theory, the resulting expressions for $\mathbb{C}_{ij}$ are calculated and given in table 1. For instance, $\mathbb{C}_{ii}$ is given by:

$$\mathbb{C}_{ii}^* = -\frac{12}{\sqrt{\pi}}(1 - e^2)\alpha_p g_0 T^{*3/2} A_1 + \frac{16}{5\sqrt{\pi}}(1 + e)\alpha_p g_0 \sqrt{T^*} A_2 - \frac{8}{5}(1 + e)\alpha_p g_0 \widehat{R}_{p,13}^*, \tag{5.5}$$

where A_1 and A_2 are monotonic functions of T^* defined by:

$$A_1(T^*) = \frac{1}{2\pi}\int_k f_{3,0}\left(\frac{k_x k_z}{\sqrt{T^*}}\right) \mathrm{d}\boldsymbol{k} \quad \text{and} \quad A_2(T^*) = -\frac{15}{4\pi}\sqrt{T^*}\int_k f_{2,0}\left(\frac{k_x k_z}{\sqrt{T^*}}\right)(k_x k_z)\, \mathrm{d}\boldsymbol{k}, \tag{5.6}$$

where $f_{n,p}(u) = \int_u^{+\infty} (x - u)^n x^p \mathrm{e}^{-x^2}\, \mathrm{d}x$ have analytical expressions. When $T^* \gg 1$, A_1 and A_2 tend to 1, leading to (5.5) having the value given by the dense ignited-state theory. On the contrary, when $T^* \ll 1$, A_1 and A_2 are equivalent to:

$$A_1 \sim_0 \frac{1}{T^{*3/2}}\frac{8}{105\sqrt{\pi}} \quad \text{and} \quad A_2 \sim_0 \frac{1}{T^{*1/2}}\frac{4}{7\sqrt{\pi}}.$$

Putting (5.7) into (5.5) leads to the value given by the dense inelastic quenched-state theory, (3.11). Hence, (5.5) is consistent with both the quenched- and ignited-state theory results. The transition between the two theories is a function of T^*, for $T^* \ll 1$ and $T^* \gg 1$ respectively. The comparison with the variations of $\mathbb{C}_{ii}^*$ and $\mathbb{C}_{33}^*$ as a function of T^* given by this theory and by the dense inelastic linear transition theory is shown on figure 6 for $e = 1$ and $\alpha_p = 0.15$. Whereas the trend for $\mathbb{C}_{ii}^*$ is similar in both theories, a wide discrepancy is found for $\mathbb{C}_{33}^*$. When $e = 1$, considering only the isotropic part of the collisional term, the dense ignited theory predicts a constant value for $\mathbb{C}_{33}^*$, whereas the new theory predicts that $\mathbb{C}_{33}^* = O(\sqrt{T^*})$ when $T^* \gg 1$. An

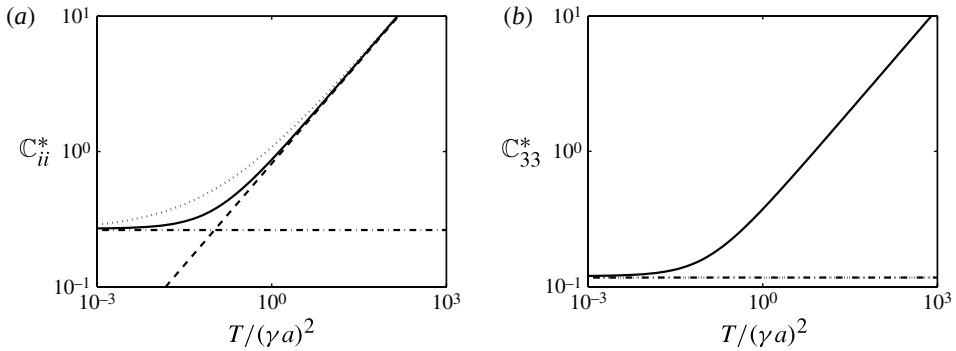

FIGURE 6. (*a*) $\mathbb{C}^*_{ii}$ and (*b*) $\mathbb{C}^*_{33}$ as functions of T^* for $e = 1$ and $\alpha_p = 0.15$: ——, nonlinear transition theory; ·····, dense linear transition theory; – – –, dense ignited-state theory; – · –·, dense quenched-state theory. Terms proportional to $\widehat{R}_{p,ij}$ are not taken into account in these plots.

analytical expression for $\mathbb{C}^*_{13}$ can be obtained and shows that this term is identical to the one obtained in the dense ignited theory.

This resulting theory is named the nonlinear transition theory.

5.2.2. *Comparison to numerical simulations*

Values of A_1, A_2, B_1 and B_2 (see table 1 and the appendix) are first numerically calculated with MATLAB and tabulated as functions of T^*. Then the numerical resolution of (3.8) is performed.

As shown on figure 1, the nonlinear transition theory is able to predict the multiple steady states observed in dilute flows and the corresponding hysteresis effects. The critical particle volume fraction predicted for $St = 10$ is $\alpha_{p,c} \simeq 1.9 \times 10^{-3}$, leading to a better agreement with numerical simulations than the linear transition theory of Tsao & Koch (1995). For $\alpha_p = 5 \times 10^{-4}$ the predicted critical Stokes number is $St_c \simeq 15.6$ which is slightly better than the value given by the linear transition theory of Tsao & Koch (1995).

In dense flows, the nonlinear transition theory matches very well the particle agitation predicted by numerical simulations for all particle volume fractions and all Stokes numbers (figure 2). Moreover the prediction of the anisotropy coefficient is very satisfactory. For $St = 5$ results are improved (figure 3). For $St = 1$, the theory leads to a perfect agreement with numerical simulations for a_{13} and the prediction of a_{33} is greatly improved.

6. Conclusion

The proposed kinetic theory approach for inertial particles suspended in a viscous sheared flow allows both shear-induced and agitation-induced inter-particle collisions to be accounted for in the kinetic stress collisional terms. The theory predictions are in very good agreement with Lagrangian simulation results from $St = 1$ to 10 and $\alpha_p = 5\,\%$ to $30\,\%$ for both the particle agitation and the anisotropy coefficients. These results show that assuming a deviated Maxwellian for the velocity distribution function leads to accurate results if both shear-induced and agitation-induced collisions are precisely taken into account.

Appendix. Functions for the nonlinear transition theory

B_1 and B_2 are functions of T^* defined by:

$$B_1(T^*) = \frac{3}{2\pi}\int_{\boldsymbol{k}} f_{3,0}\left(\frac{k_x k_z}{\sqrt{T^*}}\right) k_z^2 \,\mathrm{d}\boldsymbol{k} \quad \text{and} \quad B_2(T^*) = \frac{3}{2\pi}\int_{\boldsymbol{k}} f_{2,1}\left(\frac{k_x k_z}{\sqrt{T^*}}\right) k_z^2 \,\mathrm{d}\boldsymbol{k} \quad \text{(A 1)}$$

where $f_{n,p}(u) = \int_u^{+\infty} (x-u)^n x^p \mathrm{e}^{-x^2}\,\mathrm{d}x$ can be expressed with known functions (erf, exp, etc.). Values of A_1, A_2, B_1 and B_2 are calculated numerically with Matlab and tabulated as functions of T^*. B_1 and B_2 are defined so as to go to 1 when T^* goes to infinity. When T^* tends to zero, they become equivalent to:

$$B_1 \sim_0 \frac{1}{T^{*3/2}}\frac{32}{315\sqrt{\pi}} \quad \text{and} \quad B_2 \sim_0 \frac{4}{5\sqrt{\pi T^*}} \quad \text{(A 2)}$$

REFERENCES

ABBAS, M., CLIMENT, E., PARMENTIER, J.-F. & SIMONIN, O. 2010 Flow of particles suspended in a sheared viscous fluid: effects of finite inertia and inelastic collisions. *AIChE J.* **56** (10), 2523–2538.

ABBAS, M., CLIMENT, E. & SIMONIN, O. 2009 Shear-induced self-diffusion of inertial particles in a viscous fluid. *Phys. Rev.* E **79** (3), 36313.

BOELLE, A., BALZER, G. & SIMONIN, O. 1995 Second-order prediction of the particle-phase stress tensor of inelastic spheres in simple shear dense suspensions. In *Proceedings of the 6th International Symposium on Gas–Solid Flows,* vol. 228, pp. 9–18. ASME FED.

CARNAHAN, N. F. & STARLING, K. E. 1969 Equation of state for nonattracting rigid spheres. *J. Chem. Phys.* **51**, 635.

CHAPMAN, S. & COWLING, T. G. 1970 *The Mathematical Theory of Non-uniform Gases*. Cambridge University Press.

GRAD, H. 1949 On the kinetic theory of rarefied gases. *Commun. Pure Appl. Maths* **2** (4), 331–407.

JENKINS, J. T. & RICHMAN, M. W. 1985 Grad's 13-moment system for a dense gas of inelastic spheres. *Arch. Rat. Mech. Anal.* **87** (4), 355–377.

SANGANI, A. S., MO, G., TSAO, H. K. & KOCH, D. L. 1996 Simple shear flows of dense gas–solid suspensions at finite Stokes numbers. *J. Fluid Mech.* **313**, 309–341.

TSAO, H. K. & KOCH, D. L. 1995 Simple shear flows of dilute gas–solid suspensions. *J. Fluid Mech.* **296**, 211–246.